JOURNAL OF Applied Polymer SCIENCE

Special Issue: Microfiltration and Ultrafiltration Membrane Science and Technology

Guest Editors: Prof. Isabel C. Escobar (University of Toledo) and Prof. Bart Van der Bruggen (University of Leuven)

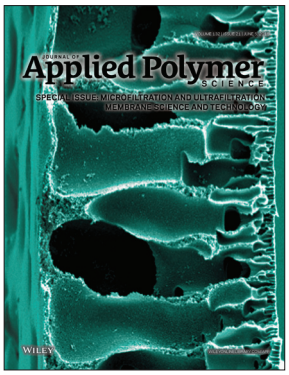

EDITORIAL

Microfiltration and Ultrafiltration Membrane Science and Technology
I. C. Escobar and B. Van der Bruggen, *J. Appl. Polym. Sci.* 2015, **DOI: 10.1002/app.42002**

REVIEWS

Nanoporous membranes generated from self-assembled block polymer precursors: *Quo Vadis*?
Y. Zhang, J. L. Sargent, B. W. Boudouris and W. A. Phillip, *J. Appl. Polym. Sci.* 2015, **DOI: 10.1002/app.41683**

Making polymeric membranes anti-fouling via "grafting from" polymerization of zwitterions
Q. Li, J. Imbrogno, G. Belfort and X.-L. Wang, *J. Appl. Polym. Sci.* 2015, **DOI: 10.1002/app.41781**

Fouling control on MF/ UF membranes: Effect of morphology, hydrophilicity and charge
R. Kumar and A. F. Ismail, *J. Appl. Polym. Sci.* 2015, **DOI: 10.1002/app.42042**

EMERGING MATERIALS AND FABRICATION

Preparation of a poly(phthalazine ether sulfone ketone) membrane with propanedioic acid as an additive and the prediction of its structure
P. Qin, A. Liu and C. Chen, *J. Appl. Polym. Sci.* 2015, **DOI: 10.1002/app.41621**

Preparation and characterization of MOF-PES ultrafiltration membranes
L. Zhai, G. Li, Y. Xu, M. Xiao, S. Wang and Y. Meng, *J. Appl. Polym. Sci.* 2015, **DOI: 10.1002/app.41663**

Tailoring of structures and permeation properties of asymmetric nanocomposite cellulose acetate/silver membranes
A. S. Figueiredo, M. G. Sánchez-Loredo, A. Maurício, M. F. C. Pereira, M. Minhalma and M. N. de Pinho, *J. Appl. Polym. Sci.* 2015, **DOI: 10.1002/app.41796**

LOW-FOULING POLYMERS

Low fouling polysulfone ultrafiltration membrane via click chemistry
Y. Xie, R. Tayouo and S. P. Nunes, *J. Appl. Polym. Sci.* 2015, **DOI: 10.1002/app.41549**

Elucidating membrane surface properties for preventing fouling of bioreactor membranes by surfactin
N. Behary, D. Lecouturier, A. Perwuelz and P. Dhulster, *J. Appl. Polym. Sci.* 2015, **DOI: 10.1002/app.41622**

PVC and PES-*g*-PEGMA blend membranes with improved ultrafiltration performance and fouling resistance
S. Jiang, J. Wang, J. Wu and Y. Chen, *J. Appl. Polym. Sci.* 2015, **DOI: 10.1002/app.41726**

Improved antifouling properties of TiO_2/PVDF nanocomposite membranes in UV coupled ultrafiltration
M. T. Moghadam, G. Lesage, T. Mohammadi, J.-P. Mericq, J. Mendret, M. Heran, C. Faur, S. Brosillon, M. Hemmati and F. Naeimpoor, *J. Appl. Polym. Sci.* 2015, **DOI: 10.1002/app.41731**

Development of functionalized doped carbon nanotube/polysulfone nanofiltration membranes for fouling control
P. Xie, Y. Li and J. Qiu, *J. Appl. Polym. Sci.* 2015, **DOI: 10.1002/app.41835**

JOURNAL OF Applied Polymer SCIENCE

Special Issue: Microfiltration and Ultrafiltration Membrane Science and Technology

Guest Editors: Prof. Isabel C. Escobar (University of Toledo) and
Prof. Bart Van der Bruggen (University of Leuven)

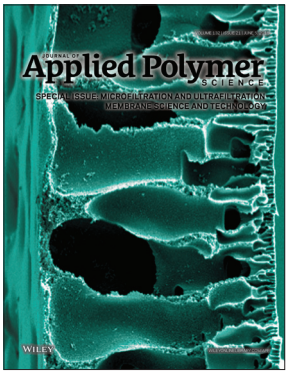

SURFACE MODIFICATION OF POLYMER MEMBRANES

Highly chlorine and oily fouling tolerant membrane surface modifications by *in situ* polymerization of dopamine and poly(ethylene glycol) diacrylate for water treatment
K. Yokwana, N. Gumbi, F. Adams, S. Mhlanga, E. Nxumalo and B. Mamba, *J. Appl. Polym. Sci.* 2015, **DOI: 10.1002/app.41661**

Fouling control through the hydrophilic surface modification of poly(vinylidene fluoride) membranes
H. Jang, D.-H. Song, I.-C. Kim, and Y.-N. Kwon, *J. Appl. Polym. Sci.* 2015, **DOI: 10.1002/app.41712**

Hydroxyl functionalized PVDF-TiO_2 ultrafiltration membrane and its antifouling properties
Y. H. Teow, A. A. Latif, J. K. Lim, H. P. Ngang, L. Y. Susan and B. S. Ooi, *J. Appl. Polym. Sci.* 2015, **DOI: 10.1002/app.41844**

Enhancing the antifouling properties of polysulfone ultrafiltration membranes by the grafting of poly(ethylene glycol) derivatives via surface amidation reactions
H. Yu, Y. Cao, G. Kang, Z. Liu, W. Kuang, J. Liu and M. Zhou, *J. Appl. Polym. Sci.* 2015, **DOI: 10.1002/app.41870**

SEPARATION APPLICATIONS

Experiment and simulation of the simultaneous removal of organic and inorganic contaminants by micellar enhanced ultrafiltration with mixed micelles
A. D. Vibhandik, S. Pawar and K. V. Marathe, *J. Appl. Polym. Sci.* 2015, **DOI: 10.1002/app.41435**

Polymeric membrane modification using SPEEK and bentonite for ultrafiltration of dairy wastewater
A. Pagidi, Y. Lukka Thuyavan, G. Arthanareeswaran, A. F. Ismail, J. Jaafar and D. Paul, *J. Appl. Polym. Sci.* 2015, **DOI: 10.1002/app.41651**

Forensic analysis of degraded polypropylene hollow fibers utilized in microfiltration
X. Lu, P. Shah, S. Maruf, S. Ortiz, T. Hoffard and J. Pellegrino, *J. Appl. Polym. Sci.* 2015, **DOI: 10.1002/app.41553**

A surface-renewal model for constant flux cross-flow microfiltration
S. Jiang and S. G. Chatterjee, *J. Appl. Polym. Sci.* 2015, **DOI: 10.1002/app.41778**

Ultrafiltration of aquatic humic substances through magnetically responsive polysulfone membranes
N. A. Azmi, Q. H. Ng and S. C. Low, *J. Appl. Polym. Sci.* 2015, **DOI: 10.1002/app.41874**

BIOSEPARATIONS APPLICATIONS

Analysis of the effects of electrostatic interactions on protein transport through zwitterionic ultrafiltration membranes using protein charge ladders
M. Hadidi and A. L. Zydney, *J. Appl. Polym. Sci.* 2015, **DOI: 10.1002/app.41540**

Modification of microfiltration membranes by hydrogel impregnation for pDNA purification
P. H. Castilho, T. R. Correia, M. T. Pessoa de Amorim, I. C. Escobar, J. A. Queiroz, I. J. Correia and A. M. Morão, *J. Appl. Polym. Sci.* 2015, **DOI: 10.1002/app.41610**

Hemodialysis membrane surface chemistry as a barrier to lipopolysaccharide transfer
B. Madsen, D. W. Britt, C.-H. Ho, M. Henrie, C. Ford, E. Stroup, B. Maltby, D. Olmstead and M. Andersen, *J. Appl. Polym. Sci.* 2015, **DOI: 10.1002/app.41550**

Membrane adsorbers comprising grafted glycopolymers for targeted lectin binding
H. C. S. Chenette and S. M. Husson, *J. Appl. Polym. Sci.* 2015, **DOI: 10.1002/app.41437**

Journal of Applied Polymer Science

Preparation of a poly(phthalazine ether sulfone ketone) membrane with propanedioic acid as an additive and the prediction of its structure

Peiyong Qin,[1] Anni Liu,[1] Cuixian Chen[2]

[1]Beijing Key Laboratory of Bioprocess, Beijing University of Chemical Technology, Beijing 100029, China

[2]Department of Chemical Engineering, Tsinghua University, Beijing 100084, China

Correspondence to: P. Qin (E-mail: qinpy@mail.buct.edu.cn)

ABSTRACT: In this study, propanedioic acid was investigated as a potential additive in poly(phthalazine ether sulfone ketone) (PPESK)/*N*-methyl-2-pyrrolidone solutions. Compared with poly(ethylene glycol) with a molecular weight of 1000 and Tween 80 as additives, different phenomena were observed: (1) both fingerlike and spongelike structures of asymmetric ultrafiltration membranes were induced by rapid gelation, and (2) a spongelike structure membrane with a high pure water flux was obtained under a high gelation rate. Moreover, the PPESK membrane formation process was recorded with a recently developed optical microscopy (OM)–charge-coupled device (CCD) camera experimental system. The predicted membrane structure with an OM–CCD system gave good correspondence with the final membrane structure and performance, as detected by scanning electron microscopy. © 2014 Wiley Periodicals, Inc. J. Appl. Polym. Sci. **2015**, *132*, 41621.

KEYWORDS: kinetics; membranes; separation techniques

Received 28 July 2014; accepted 15 October 2014

DOI: 10.1002/app.41621

INTRODUCTION

Bioenergy has attracted more and more attention because of a crude oil crisis. Separation technology is a big challenge in bioenergy production, especially biomass pretreatment. There are considerable needs of membranes with different structures,[1–3] so membrane structural prediction is important for membrane preparation.

Since Loeb and Sourirajan[4] exploited the preparation method of ultrafiltration membranes via a wet phase-inversion process, the mechanism of membrane formation has been widely studied. Young and Chen[5] thought it was solvent–nonsolvent–polymer interactions that led to the asymmetric structure of ultrafiltration membranes. Numerous investigations on the gelation kinetics were also developed by Strathmann *et al.*[6] A plot of the square value of the movement of the precipitation front (X^2) against time, may lead to a kinetic model ($X^2=4\bar{D}\frac{\epsilon}{\tau}\times\frac{1-C_P}{1+C_P}\cdot t$) in which $\bar{D}$ is the average diffusion coefficient of the nonsolvent gelation process, ϵ represents the porosity, τ is the membrane tortuosity, and C_P is the concentration of nonsolvent in the liquid phase at the point of precipitation. With the assumption that the cross section of the membrane has the same porosity and pore tortuosity, the conclusions based on the previously model were as follows:

1. A finger-structure membrane was obtained via the rapid gelation method, whereas a sponge-structure membrane was obtained under a slower gelation rate.
2. The water flux of the finger-structure membrane was larger than that of the sponge-structure membrane.

In our previous research,[7–11] poly(ethylene glycol) with a molecular weight of 1000 (PEG1000) and Tween80 were already investigated. Both PEG1000 and Tween80 as potential additives displayed the same tendencies shown in the previous conclusions.

With an optical microscopy (OM) photography technique, Yong *et al.*[12,13] further confirmed the two conclusions based on the previous kinetic model. The precipitation front moved very fast in the first period, especially within the first 10 s. It was very difficult to record the moved distance of the precipitation front because they run the experiments with a relatively lower precision of instruments. To monitor the process of membrane formation, the equipment was improved by our previous

Additional Supporting Information may be found in the online version of this article.

research.[7–11] Compared with Strathmann's results, three different linear correlations were obtained; these corresponded to formation of the skin layer, the transition layer, and the finger layer, respectively.[7] Clearly, the three layers of membrane showed different porosities and pore tortuosities. So, the membrane structure prediction with Strathmann's experiments did not work perfectly.

Oxalic acid (OA) was able to strongly enhance the gelation rate of the Poly(phthalazine Ether Sulfone) (PPES) membrane formation and improve the PPES membrane structure because of the two COOH group in its molecular structure.[9] Propanedioic acid (PA), also as a dicarboxylic acid, can act as a good hydrogen donor through the COOH group. Maybe it can also enhance the gelation rate of membrane formation and improve the membrane performance and structure. In this study, PA was selected as an additive to prepare poly(phthalazine ether sulfone ketone) (PPESK) membranes. Also, an attempt was made to compare the picture captured by the OM–charge-coupled device (CCD) system with the scanning electron microscopy (SEM) picture of the membrane cross section. The results may provide a guide for the PPESK membrane preparation.

EXPERIMENTAL

Materials

PPESK with a molecular weight of 218,900 was obtained from Dalian Polymer New Material Co., Ltd. (Liaoning Province, China). *N*-Methyl pyrrolidone (NMP) as a solvent and poly(vinyl pyrrolidone) (PVP; K30) and PA as nonsolvent additives were obtained from Beijing Yili Fine Chemicals Co., Ltd. (Beijing, China).

Preparation of the Flat Membranes

PPESK membranes were prepared by a phase-inversion method. A certain quality of PPESK, additives, and solvent were injected into a grinding mouth flask, and the mixture was dissolved for 72 h in a shaker at 60°C. The casting solution was filtered and vacuumed to remove bubbles. The flat ultrafiltration membrane was prepared by the casting of polymer solution onto nonwoven fabrics that were 120 μm thick at 20°C with about 20–40% humidity. The coated nonwoven fabrics where then immediately immersed into a 25°C coagulation bath. Finally, the fresh membrane was stored in a dilute formalin solution after solvent extraction.

Characterization of the Membrane

The ultrafiltration membrane was first immersed in distilled water to eliminate the formalin influence. SEM observation was done and the pure water flux and bovine serum albumin (BSA) rejection of PPESK membrane were measured according to our previous article.[9] SEM was done on a Cambridge S-250 field emission scanning electron microscope (Cambridge, Inc., United Kingdom). The pure water flux was determined with distilled water at 0.1 MPa and 25°C. A concentration of 400 mg/L of BSA solution was used to characterize the PPESK membrane rejection at 0.1 MPa and 25°C. The BSA concentration was measured at a wavelength of 280 nm with a UV spectrophotometer (model UV-2102 PCS, Unico). The viscosity of the PPESK casting solution was determined at 25°C with a Brookfield DV-II+CP viscometer (Brookfield, Middleboro, MA). The online OM–CCD camera system was used to determinate the gelation rate and observe the membrane structural evolution process.[11] About 10 μL of the PPESK casting solution was introduced into two specially designed accessories of the microscope. A volume of 1 mL of distilled water was used as coagulant to be rejected into a compartment with two syringes. The images during membrane formation were automatically taken by a CCD camera at 12 frames per second. The precipitated thickness of the PPESK membrane was measured by Image J software (Image J, National Institute of Mental Health, Bethesda, MD,). All data represent the average values of three repeated experiments with less than a plus or minus 5% deviation.

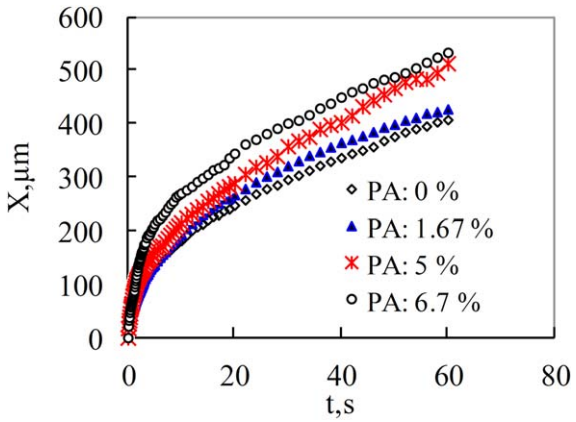

Figure 1. Effect of the PA concentration as an additive on the gelation rate in PPESK/NMP at 25°C (concentration of PPESK = 15.6%). X is the movement of the precipitation front. [Color figure can be viewed in the online issue, which is available at wileyonlinelibrary.com.]

Cloud Point

The cloud points were determined by a titration method.[14] The ratio of PPESK to the additives was 5:4. A series of samples with 1–10 wt % PPESK and additives were dissolved in NMP with a water bath at 70°C until a homogeneous solution was obtained. Then, the solutions were cooled to 25°C. Distilled water was added little by little to the solutions and mixed. The composition of the cloud point was obtained when the solution was just visually turbid.

RESULTS AND DISCUSSION

Influence of the PA Additive on the PPESK Ultrafiltration Membranes

To compare PA with PEG1000 and Tween80 as additives, which were already investigated in our previous study,[11] the same concentrations of PA (0, 1.67, 5, and 6.7%) were selected. PPESK/NMP at 15.6 wt % was used as the casting solution, whereas deionized (DI) water was the nonsolvent. Figure 1 shows the gelation rate of the PPESK casting solution precipitated in DI water with PA as the additive. PA enhanced the hydrophilicity of the PPESK casting solution, and the gelation rate of the PPESK casting solution increased with the PA concentration. At a PA concentration of 6.7%, the gelation rate reached a maximum value. However, when the PA concentration was greater

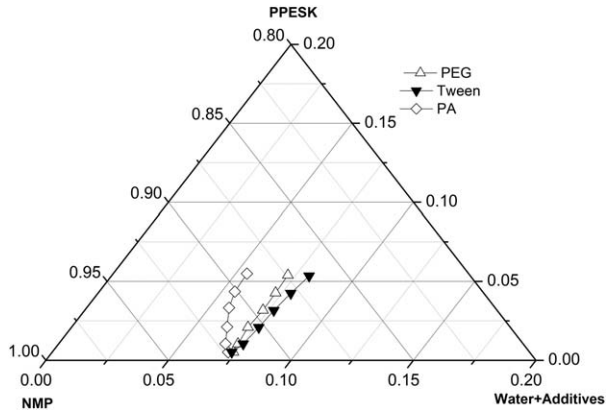

Figure 2. Effect of additives on the cloud point of PPESK/NMP/water at 25°C.

than 7%, PPESK/PA/NMP could not form a homogeneous casting solution.

Figure 2 shows the cloud points of the PPESK solution with PA, PEG1000, and Tween80 as additives, respectively. Clearly, with the addition of PA, the binodal line shifted more toward the solvent–polymer axis than those of PEG1000 or Tween80. The shift led to a decrease in the stable one-phase region and increases in the unstable and metastable regions. Thus, PA addition caused the casting solution system to be less thermodynamically stable than those of PEG1000 or Tween80 as additives, and this led to a fast phase separation.

To clearly show the evolution of the membrane structure as the PA concentration was increased, a cross section of the PPESK membranes was observed by OM–CCD, as shown in Figure 3. The figures show that as the PA content increased, the fingerlike structure was gradually transformed to a spongelike structure. The spongelike structure was totally formed when the PA concentration was 6.7%. Interestingly, as the PA concentration increased, the water flux of the membranes increased. The water fluxes of the membranes with 0, 1.67, 5, and 6.7% PA were 240, 469, 500, and 580 L $m^{-2}{\cdot}h^{-1}$, respectively. The water flux reached a maximum value at 6.7% PA. The SEM micrographs of the PPESK membrane cross sections are presented in Figure 4. They also showed an asymmetric structure and exhibited the same regulation as the optical microscopy (OM) pictures show in Figure 3.

Figure 5 shows some images of PPESK membrane formation obtained with the OM–CCD system. When the membranes

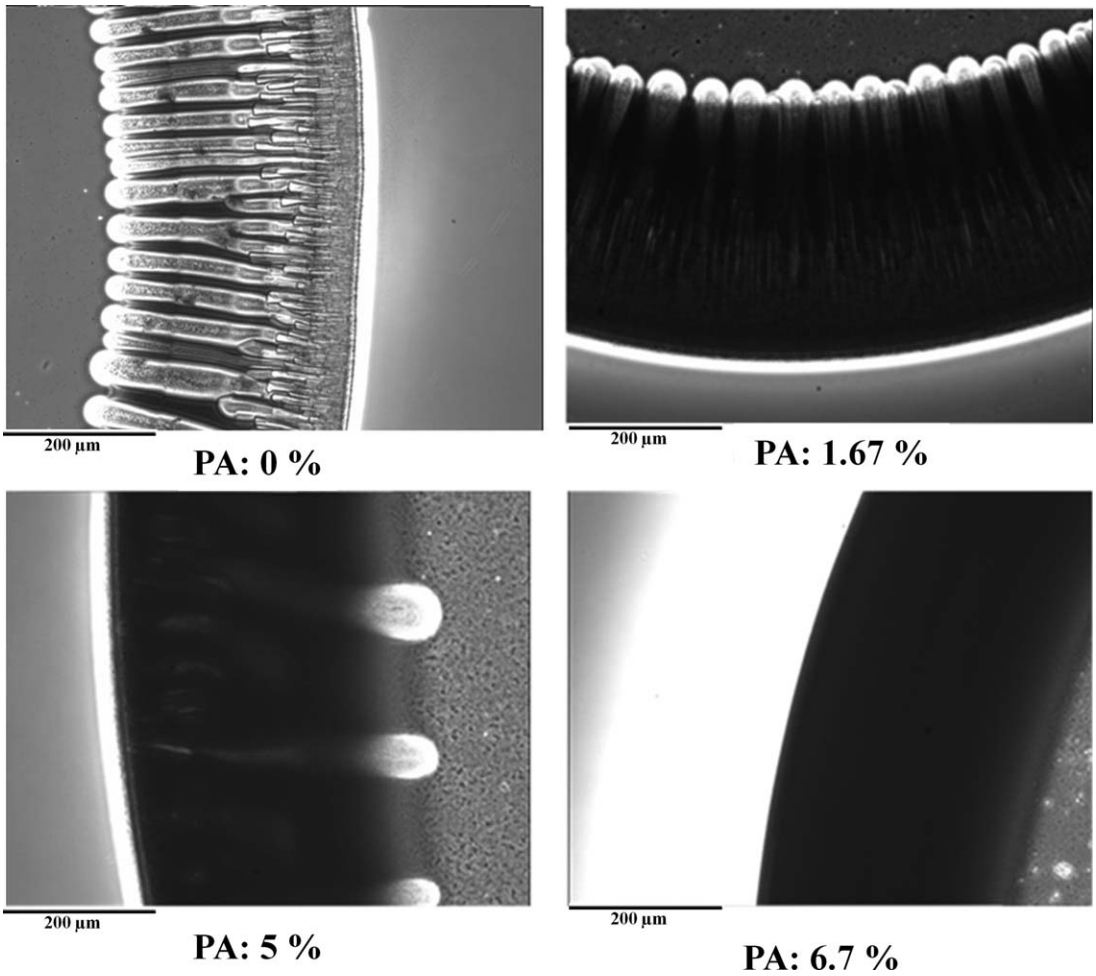

Figure 3. Optical micrograph of the membrane prepared by the variation of the PA concentration as an additive in PPESK/NMP at 25°C (concentration of PPESK = 15.6%).

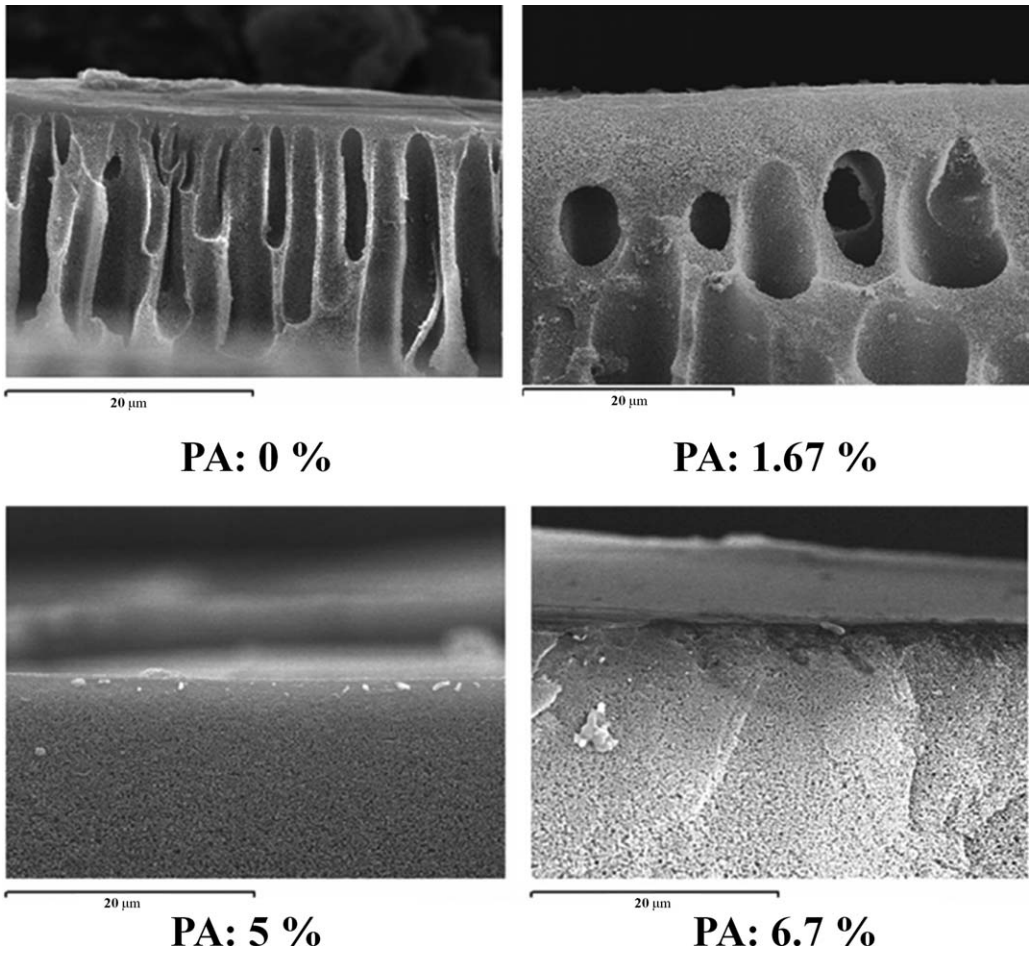

Figure 4. SEM of the membranes prepared by the variation of the PA concentration at 25°C (concentration of PPESK = 15.6%).

with 6.7% PA (A1–A6) were compared with the control group (B1–B6) at various precipitated times, we observed that a fingerlike membrane was obtained without PA addition, whereas a spongelike membrane was observed at a 6.7% PA concentration with a higher rapid gelation rate. After 40 s of precipitation, three layers of PPESK membrane were clearly distinguished, including a dense top layer, a transition layer, and a support layer.

As shown in Figure 5, the spongelike structure formed more quickly than the finger structure. Because the molecular structure of PA was similar to that of OA, also including two COOH groups, PA as an additive should have played the same role as OA during the PPESK membrane formation.[9] Hydrogen bonds could be formed between PA and NMP through the C═O as a hydrogen-bond acceptor in NMP and the COOH group as a hydrogen donor in PA.[9] The amount of free molecular NMP in the polymer solution decreased because of hydrogen-bond formation; this enhanced the phase separation of the PPESK membrane solution. Also, PA and PPESK formed a bridge complex through the two ─OH groups in PA and the carbonyl and nitrogen groups of PPESK.[9] The high rigid molecular structure of the bridge complex resulted in a low PPESK solubility. Moreover, the phase-separation rate of the polymer solution increased because of the steric hindrance. Like OA, PA also showed strong hydrophilic characteristics, and water vapor in the atmosphere easy diffused into the polymer solution; this accelerated the microphase formation. As shown in Figure 5(A1), two phases, a polymer-rich phase and a polymer-poor phase, were formed before the nonsolvent was introduced into the polymer solution. All of the previous factors led to a high flux and rapid phase separation during PPESK membrane formation. It is well known that delayed liquid–liquid demixing will cause spongelike structure formation and that instantaneous demixing will result in a fingerlike structure. However, when the component of the casting solution was near biondal; the polymer solution system was highly thermodynamically unstable, and when very little coagulant (water vapor in air) was introduced into the system, it resulted in microphase separation [Figure 5(A1)]. When the microphase system was immersed in coagulant, the casting solution system would pass through the metastable region with a very fast speed and cause spinodal demixing. Thus, a spongelike structure was obtained.

In fact, the viscosity also played an important role. The viscosities of the casting solutions with 0, 1.67, 5, and 6.7% PA were determined with 1162, 1540, 2630, and 3453 cP, respectively.

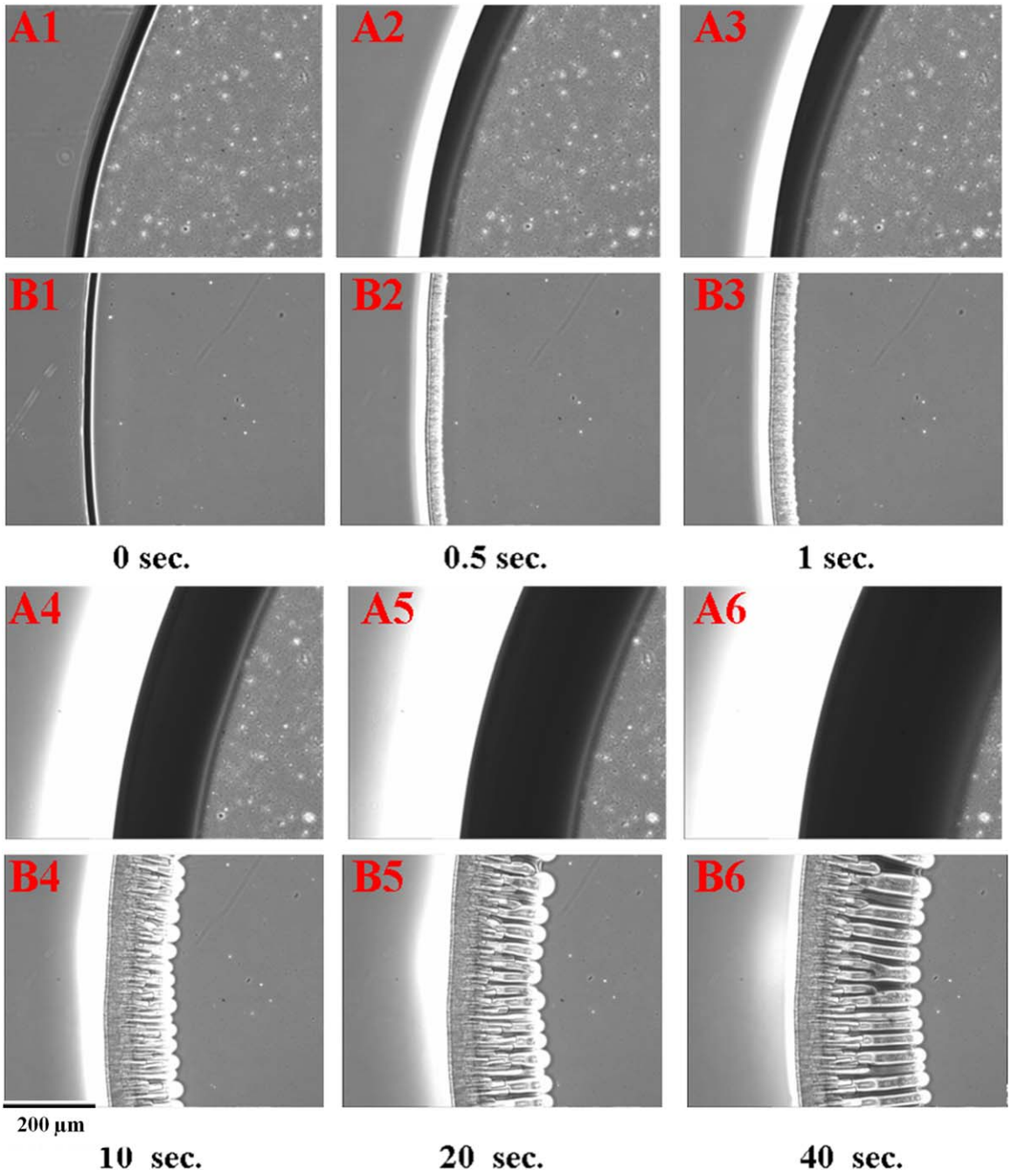

Figure 5. Membrane cross-sectional structure evolution with the precipitated time at 25°C (A1–A6: 6.7% PA, B1–B6: 0% propanedioic as an additive). A concentration of 15.6 wt % PPESK/NMP was used as the polymer solution, whereas DI water was the nonsolvent. [Color figure can be viewed in the online issue, which is available at www.interscience.wiley.com.]

The drastic increasing viscosity slowed down the solvent outflow and nonsolvent penetration rate. The slow diffusion rate provided enough time for the rich phase to coalesce and, thus, form denser top layers; this resulted in a high BSA rejection.

As strong hydrophilic additives, the added PA resulted in a less thermodynamically stable and enhanced gelation rate; this was pronounced compared to the effects of the viscosity increase. Therefore, a finger pore could not form at this fast phase separation. A spongelike structure formed with the rapid gelation rate.

The pK_{a1} and pK_{a2} of PA were 2.85 and 5.70, respectively. Although the pK_{a1} and pK_{a2} of OA were 1.27 and 4.27, respectively. PA was less acidic than OA; this will result in a weak ability for hydrogen-bond formation for PA compared with OA. PA also shows less hydrophilicity than OA because of its long carbon chain. All of these decreased the phase-separation rate compared with OA as an additive. However, the molecular structure of PPESK was more rigid than that of PPES. It was also interesting that the membrane structure evolution from a

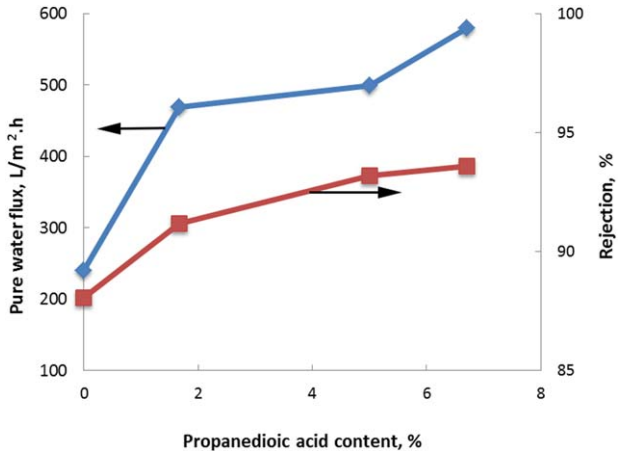

Figure 6. Pure water flux and BSA rejection of the PPESK membrane as a function of the PA content. [Color figure can be viewed in the online issue, which is available at wileyonlinelibrary.com.]

fingerlike structure to a spongelike structure was easier for the PPESK membrane than the PPES membrane. The spongelike structure of the PPESK membrane was found at 5% PA, whereas the spongelike structure of the PPES membrane was formed at 10% OA. These results show that a high rigid molecular structure also enhanced the phase separation and spongelike structure formation. We concluded that polymer molecular conformation also played an important role in the membrane structural evolution.

Figure 6 shows the pure water flux and BSA rejection of the PPESK membrane. Like with the PPES membrane with OA as an additive, the pure water flux and BSA rejection of the PPESK membrane also exhibited a positive correlation with the PA concentration. Because of the strong hydrophilicity of PA, the casting solution exhibited a high thermodynamic instability and reached a critical state. Even a small amount of water vapor permeation into the casting solution caused microphase separation. Moreover, the increasing viscosity of the casting solution prevented water vapor from rapidly crossing the skin layer and going deep into the casting solution. The high viscosity of the casting solution also resulted in a small pore size in the top skin layer; this led to a high BSA rejection. The casting solution system with PA as an additive showed a higher gelation rate and a large number of microphase zone [Figure 5(A1)] during membrane formation; this resulted in a high porosity in the top skin layer of the PPESK membrane. In this case, the PPESK membrane exhibited a high water flux and rejection. The pure water flux of the PPESK membrane was about 500 L m^{-2} h^{-1}, and its membrane structure was spongelike when the concentration of PA was 5%, whereas the pure water flux of the PPES membrane was only about 300 L m^{-2} h^{-1} and its membrane structure was fingerlike when the concentration of OA was 5%.[9] The BSA rejection of the PPESK membrane increased from 85 to 95% with increasing additive content, whereas the BSA rejection of the PPES membrane was more than 96%.[9] The high rigid molecular structure of PPESK led to a higher flux and lower BSA rejection than those found in the PPES membrane.

Some articles have already reported the relationship between the gelation rate and the membrane structure.[15] It was noted that the gelation rate of the fingerlike structure membrane was faster than that of the spongelike structure membrane.[16] Thus, rapid gelation led to a fingerlike structure formation, whereas slow gelation resulted in a spongelike structure membrane. At the same time, the relationship between the membrane structure and performance was also investigated. It was considered that the water flux of the fingerlike structure membrane was larger than that of the spongelike structure membrane. Strathmann and coworkers[6,17–19] confirmed these conclusions via a set of photographs, which agreed with the conclusions of other scholars.[20,21]

In our earlier research,[11] two additives, PEG1000 and Tween80, were used. The gelation rate showed the same variation trend with the membrane flux change. The same conclusions were reached as those of Strathmann and coworkers.[6,17–19] However, phenomena different from those observed by other scholars were obtained when PA or OA was used as an additive. These were as follows:

1. Both the fingerlike structure membrane and the spongelike structure membrane could be induced by rapid gelation method.
2. The water flux of the spongelike structure membrane was larger than that of fingerlike structure membrane.

From results in an PPES/NMP/OA solution in our previous study[9] and PPESK/NMP/PA solution in this study, the previous conclusions were obtained when the additive with a strong hydrophilicity accelerated the microphase separation of the membrane skin layer when the casting polymer solution was exposed to the atmosphere.

Predication of the Membrane Structure by OM Imagery

The prediction of the membrane performance and structure is still a big challenge in membrane preparation. Membrane formation was observed with the online OM–CCD camera experimental system (OM–CCD), whereas SEM was used to observe the actual cross section of the membranes.

When the SEM image in Figure 4 was compared with the photograph taken from the online OM–CCD camera experimental system in Figure 3, the membrane structure observed on the OM–CCD exhibited almost the same cross section with that observed with SEM. Figure 7 compares the SEM images of four classical membrane structures with their OM images taken from OM–CCD. The results show that OM images and the final membrane structures (SEM) were in good agreement. These indicated that the membrane formation process observed with OM–CCD was almost the same as the actual membrane formation. The photos in Figure 7 clearly show that the membrane structure was composed of a skin layer, a transition layer, and a finger/sponge layer. As shown in Figure 7(A1,B1), a fingerlike structure membrane, which often had a high flux, was obtained with 2.5% PA as an additive in PPESK/NMP. When the PA concentration increased to 7.5%, the membrane structure was obviously transformed to a spongelike structure, as shown in Figure 7(A3,B3). A concentration of 18%

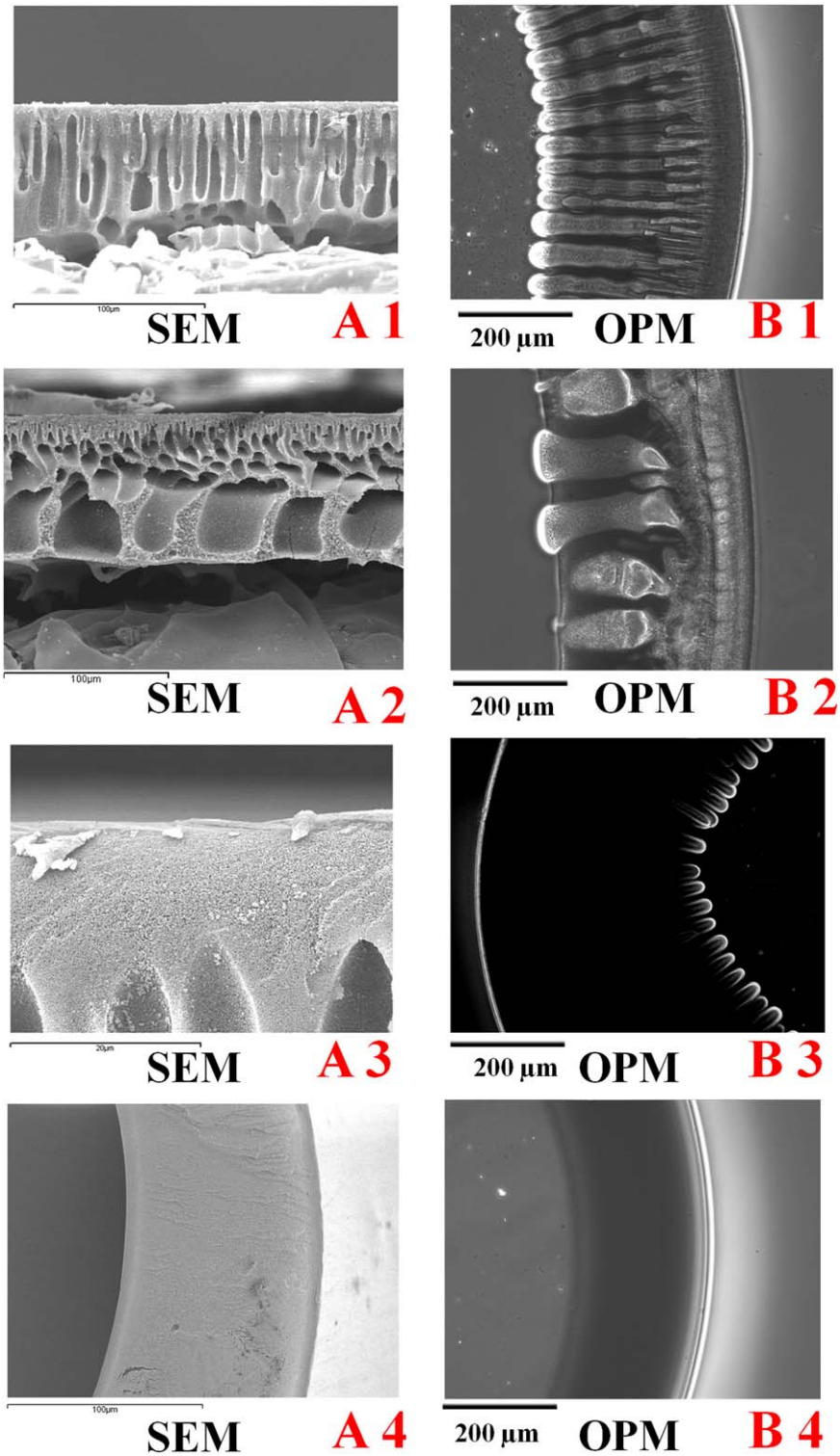

Figure 7. Cross sections of the membranes images under different conditions taken by both (A) SEM and (B) OM (OPM, optical micrograph images). (A1,B1) 18 wt % PPESK/NMP was used as the polymer solution. A concentration of 2.5% PA was used as an additive at 60°C. (A2,B2) 18 wt % polysulfone (PSF)/NMP was used as the polymer solution at 60°C. (A3,B3) 18 wt % PPESK/NMP was used as the polymer solution. A concentration of 7.5% PA was used as additive at 60°C. (A4,B4) 18 wt % PPESK/NMP was used as the polymer solution. A concentration of 7.5% PVP was used as additive at 25°C. [Color figure can be viewed in the online issue, which is available at wileyonlinelibrary.com.]

polysulfone (PSF) induced nonuniform macrovoid formation, as displayed in Figure 7(A2,B2). Moreover, as shown in Figure 7(A4,B4), the spongelike structure was totally formed with 7.5% PVP as an additive.

The OM photos and SEM pictures were in good agreement and indicated that the gelation rate and OM images obtained from the OM–CCD system could be used to guide membrane preparation to quickly obtain excellent membrane performance and structure.

CONCLUSIONS

Novel phenomena were observed when PA was used as an additive to prepare PPESK membranes. PA, as a strong hydrophilic additive, made the casting solution reach a critical state. At this state, PA led to the microphase separation of the membrane skin layer and enhanced the gelation rate of the PPESK membrane formation. In case of microphase separation and a fast gelation rate, the spongelike structure membrane exhibited a higher flux than the fingerlike structure membrane. Polymer molecular conformation also played an important role in the membrane structure evolution. OM images obtained from OM–CCD were used to predict the membrane structure.

ACKNOWLEDGMENTS

The authors are grateful to the National Basic Research Program of China (contract grant number 2013CB733600) and for the financial support received from National Nature Science Foundation of China (contract grant numbers 21276017 and 21476015). They also acknowledge the contribution of Nazmul. M. Karim at Texas A&M University, who professionally reviewed the article and helped them to improve their English.

REFERENCES

1. Abels, C.; Thimm, K.; Wulfhorst, H.; Spiess, A. C.; Wessling, M. *Bioresour. Technol.* **2013**, *149*, 58.
2. Pilath, H. M.; Michener, W. E.; Katahira, R.; Mittal, A.; Clark, J. M.; Himmel, M. E.; Johnson, D. K. *Energy Fuel* **2013**, *27*, 7389.
3. Gassner, M.; Maréchal, F. *Energy Fuel* **2013**, *27*, 2107.
4. Loeb, S.; Sourirajan, S. *Adv. Chem. Ser.* **1963**, *38*, 117.
5. Young, T. H.; Chen, L. W. *J. Membr. Sci.* **1993**, *83*, 153.
6. Strathmann, H.; Kock, K.; Amar, P.; Baker, R. W. *Desalination* **1975**, *16*, 179.
7. Qin, P.; Han, B.; Chen, C.; Takuji, S.; Li, J.; Sun, B. *Desalin. Water Treat.* **2009**, *11*, 157.
8. Yun, Y.; Le-Clech, P.; Dong, G.; Sun, D.; Wang, Y.; Qin, P.; Chen, C. *J. Membr. Sci.* **2012**, *389*, 416.
9. Qin, P.; Hong, X.; Karim, M. N.; Shintani, T.; Li, J.; Chen, C. *Langmuir* **2013**, *29*, 4167.
10. Qin, P.; Han, B.; Chen, C.; Li, J.; Sun, B. *Korean J. Chem. Eng.* **2008**, *25*, 1407.
11. Qin, P.; Chen, C.; Han, B.; Takuji, S.; Li, J.; Sun, B. *J. Membr. Sci.* **2006**, *268*, 181.
12. Yao, C. W.; Burford, R. P.; Fane, A. G.; Fell, C. J. D. *J. Membr. Sci.* **1988**, *38*, 113.
13. Yong, S. K.; Hyo, J. K.; Un, Y. K. *J. Membr. Sci.* **1991**, *60*, 219.
14. Lau, W. W. Y.; Guiver, M. D.; Matsuura, T. *J. Membr. Sci.* **1991**, *59*, 219.
15. Pires Vilela, J. A.; Cavallieri, Â. L. F.; Lopes da Cunha, R. *Food Hydrocolloids* **2011**, *25*, 1710.
16. Kimmerle, K.; Strathmann, H. *Desalination* **1990**, *79*, 283.
17. Strathmann, H. *ACS Symp. Ser.* **1985**, *269*, 165.
18. Strathmann, H.; Kock, K. *Desalination* **1977**, *21*, 241.
19. Strathmann, H. *J. Membr. Sci.* **1981**, *9*, 121.
20. Kim, H. J.; Tyagi, R. K.; Fouda, A. E.; Jonasson, K. *J. Appl. Polym. Sci.* **1996**, *62*, 621.
21. Frommer, M. A.; Lancet, D. In Reverse Osmosis Membrane Research; Lonsdale, H. K., Podall, H. E., eds.; Plenum: New York, **1972**; p 85.